

# Neutral Current Coherent Cross Sections- Implications on Gaseous Spherical TPC's for detecting SN and Earth neutrinos

J. D. Vergados<sup>1\*</sup> and Y. Giomataris<sup>2</sup>

*ARC Centre of Excellence in Particle Physics at the Terascale and Centre for the Subatomic Structure of Matter (CSSM), University of Adelaide, Adelaide SA 5005, Australia, <sup>1</sup>, <sup>2</sup> IRFU, CEA, Université Paris-Saclay, F-91191 Gif-sur-Yvette, France*

The detection of galactic supernova (SN) neutrinos represents one of the future frontiers of low-energy neutrino physics and astrophysics. The neutron coherence of neutral currents (NC) allows quite large cross sections in the case of neutron rich targets, which can be exploited in detecting earth and sky neutrinos by measuring nuclear recoils. They are relatively cheap and easy to maintain. These (NC) cross sections are not dependent on flavor conversions and, thus, their measurement will provide useful information about the neutrino source. In particular they will yield information about the primary neutrino fluxes and perhaps about the spectrum after flavor conversions in neutrino sphere. They might also provide some clues about the neutrino mass hierarchy. The advantages of large gaseous low threshold and high resolution time projection counters (TPC) detectors TPC detectors are discussed.

PACS numbers: 21., 95.35.+d, 12.60.Jv

## I. INTRODUCTION

The detection of galactic supernova (SN) neutrinos represents one of the future frontiers of low-energy neutrino physics and astrophysics. In this paper we are going to discuss the relevant physics for the design and construction of a gaseous spherical TPC for dedicated supernova detection, exploiting the coherent neutrino-nucleus elastic scattering due to the neutral current interaction. This detector can draw on the progress made in recent years in connection with measuring nuclear recoils in dark matter searches. It has low threshold and high resolution, it is relatively cheap and easy to maintain. Before doing this, however, we will briefly discuss the essential physics of neutrinos emitted in supernova explosions [1] (for a review, see, e.g. the recent report [2])

## II. THE SUPERNOVA NEUTRINO FLUX.

We will assume that the neutrino spectrum can be described by a Fermi Dirac Distribution with a given temperature  $T$  and a chemical potential  $\mu = aT$ . The constants  $T$  and  $a$  will be treated as free parameters. Thus

$$f_{sp}(E_\nu, T, a) = \mathcal{N} \frac{1}{1 + \exp(E_\nu/T - a)} \quad (1)$$

where  $\mathcal{N}$  is a normalization constant. The temperature  $T$  is taken to be 3.5, 5 and 8 MeV for electron neutrinos ( $\nu_e$ ), electron antineutrinos ( $\bar{\nu}_e$ ) and all other flavors ( $\nu_x$ ) respectively. The parameter  $a$  will be taken to be  $0 \leq a \leq 5$ . The average neutrino energies obtained from this distribution are shown in Table I.

The number of emitted neutrinos [1] can be obtained from the total emitted energy  $U_\nu = 3 \times 10^{53}$  erg

$$N_\nu = \frac{U_\nu}{\langle E_\nu \rangle}. \quad (2)$$

The obtained results are shown in Table II The (time averaged) neutrino flux  $\Phi_\nu = N_\nu/(4\pi D^2)$  at a distance  $D = 10$  kpc= $3.1 \times 10^{22}$ cm is given in Table III.

## III. MODIFICATION OF THE SRN SPECTRA DUE TO NEUTRINO OSCILLATION OSCILLATION

Even though the neutral current detector is neutrino flavor bound, the neutrino oscillations modify the SRN spectrum. This modification will affect the expected rates since the different flavors have different temperature and

---

\* Permanent address: Theoretical Physics, University of Ioannina, Ioannina, Gr 451 10, Greece.

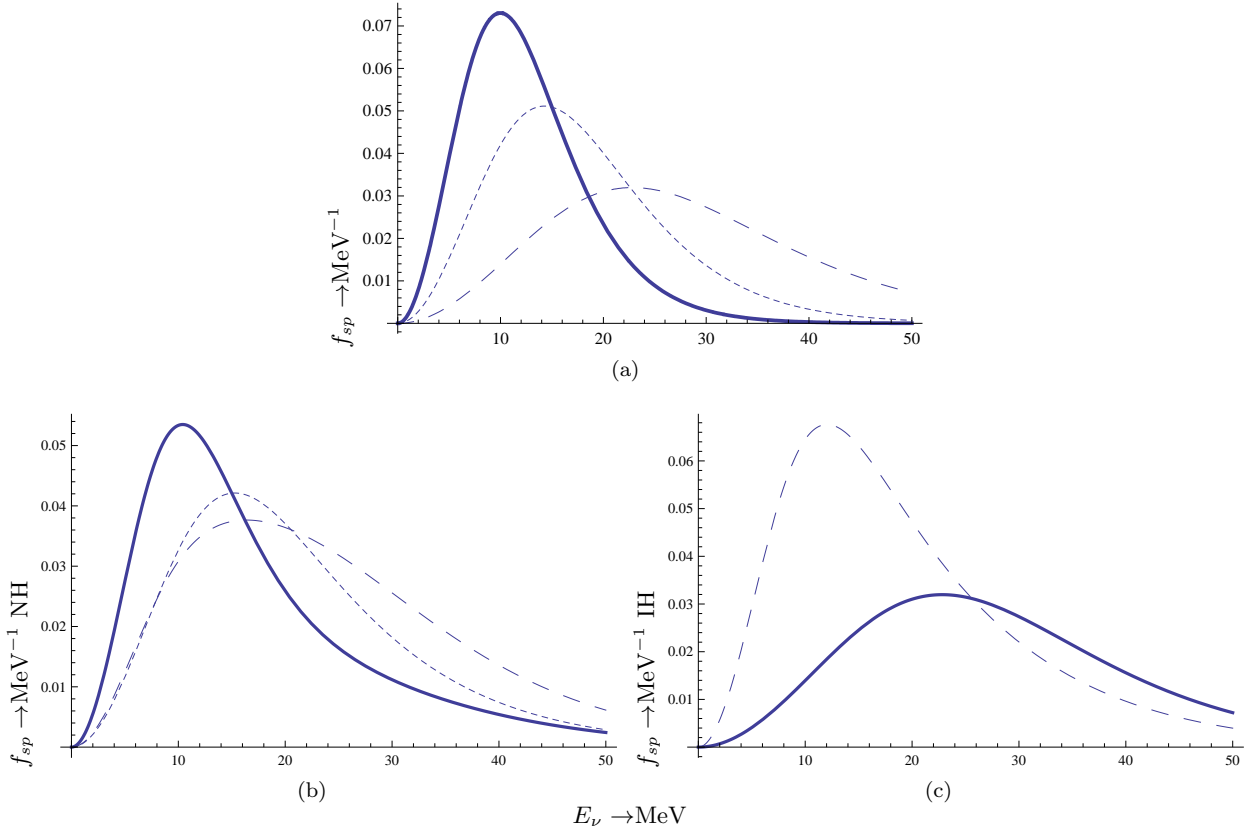


Figure 1: The normalized to unity SN spectrum for  $a = 3$  (a) and the modified SN spectra also for  $a = 3$  in the normal hierarchy scenario (b) and the inverted hierarchy scenario (c). The continuous, dotted and dashed curves correspond to  $T=3.5$  ( $\nu_e$ ), 5 ( $\tilde{\nu}_e$ ) and 8 ( $\nu_x$ ) respectively. In the case of the inverted hierarchy scenario the spectra for  $\nu_e$  and  $\tilde{\nu}_e$  coincide

Table I: The average supernova neutrino energies as a function of the parameters  $a$  and  $T$ .

$a$	$\langle E_\nu \rangle$ (MeV)		
	$\nu_e$ T=3.5MeV	$\tilde{\nu}_e$ T=5MeV	$\sum_x \nu_x$ T=8MeV
0	11.0298	15.7569	25.211
0.75	11.4504	16.3578	26.1724
1.50	12.0787	17.2553	27.6085
2.00	12.6194	18.0277	28.8443
3.00	13.9733	19.9619	31.9391
4.00	15.6313	22.3305	35.7288
5.00	17.5179	25.0255	40.0408

chemical potential. This modification has recently been discussed [3], [4]. Neutrino oscillations imply:

$$\frac{dN_{\nu_e}}{dE_\nu} = U_{e1}^2 \frac{dN_{\nu_1}}{dE_\nu} + U_{e2}^2 \frac{dN_{\nu_2}}{dE_\nu} + U_{e3}^2 \frac{dN_{\nu_3}}{dE_\nu} \quad (3)$$

$$\frac{dN_{\nu_x}}{dE_\nu} = U_{x1}^2 \frac{dN_{\nu_1}}{dE_\nu} + U_{x2}^2 \frac{dN_{\nu_2}}{dE_\nu} + U_{x3}^2 \frac{dN_{\nu_3}}{dE_\nu}, \quad x = \mu, \tau \quad (4)$$

Table II: The number of primary neutrinos emitted in a typical supernova explosion as a function of the parameters  $a$  and  $T$  in units of  $10^{58}$ .

$a$	$N_\nu/10^{58}$		
	$\nu_e$ T=3.5 MeV	$\bar{\nu}_e$ T=5 MeV	$\sum_x \nu_x$ T=8 MeV
0	0.282969	0.198079	0.495196
0.75	0.272575	0.190802	0.477006
1.50	0.258397	0.180878	0.452194
2.00	0.247326	0.173128	0.43282
3.00	0.223361	0.156353	0.390882
4.00	0.199669	0.139768	0.349421
5.00	0.178167	0.124717	0.311792

Table III: The (time integrated) neutrino flux, in units of  $10^{12}\text{cm}^{-2}$ , at a distance 10 kpc from the source.

$a$	$\Phi_\nu/10^{12}\text{cm}^{-2}$		
	$\nu_e$ T=3.5 MeV	$\bar{\nu}_e$ T=5 MeV	$\sum_x \nu_x$ T=8 MeV
0	0.234318	0.164023	0.410057
0.75	0.225711	0.157997	0.394994
1.50	0.213971	0.149779	0.374448
2.00	0.204803	0.143362	0.358405
3.00	0.184958	0.129471	0.323677
4.00	0.16534	0.115738	0.289345
5.00	0.147534	0.103274	0.258185

for neutrinos and antineutrinos. The superscript zero refers to the primary neutrino spectra. It can be shown that for the normal hierarchy  $m_1 < m_2 < m_3$

$$\frac{dN_{\nu_1}}{dE_\nu} \approx \frac{dN_{\nu_e}^0}{dE_\nu}, \frac{dN_{\nu_2}}{dE_\nu} \approx \frac{dN_{\nu_x}^0}{dE_\nu}, \frac{dN_{\nu_3}}{dE_\nu} \approx \frac{dN_{\nu_x}^0}{dE_\nu} \text{ NH}, \quad (5)$$

while for the inverted hierarchy (IH)  $m_3 < m_2 < m_1$  these equations become:

$$\frac{dN_{\nu_1}}{dE_\nu} \approx \frac{dN_{\nu_x}^0}{dE_\nu}, \frac{dN_{\nu_2}}{dE_\nu} \approx \frac{dN_{\nu_x}^0}{dE_\nu}, \frac{dN_{\nu_3}}{dE_\nu} \approx \frac{dN_{\nu_e}^0}{dE_\nu} \text{ IH}, \quad (6)$$

Combining these equations we get for NI:

$$\frac{dN_{\nu_e}}{dE_\nu} \approx \frac{2}{3} \frac{dN_{\nu_e}^0}{dE_\nu} + \frac{1}{3} \frac{dN_{\nu_x}^0}{dE_\nu}, \frac{dN_{\nu_x}}{dE_\nu} \approx \frac{1}{6} \frac{dN_{\nu_e}^0}{dE_\nu} + \frac{5}{6} \frac{dN_{\nu_x}^0}{dE_\nu}, \quad (7)$$

while for the IH we find:

$$\frac{dN_{\nu_e}}{dE_\nu} \approx \frac{dN_{\nu_x}^0}{dE_\nu}, \frac{dN_{\nu_x}}{dE_\nu} \approx \frac{1}{2} \left( \frac{dN_{\nu_e}^0}{dE_\nu} + \frac{dN_{\nu_x}^0}{dE_\nu} \right). \quad (8)$$

For completeness we mention that as the neutrinos continue to propagate outwards, they encounter a further modification by the Mikheyev-Smirnov-Wolfenstein (MSW) effect [5], [6]. It has been shown [7] that

$$\begin{aligned} \frac{dN_{\nu_e}''}{dE_\nu} &\approx P_m \frac{dN_{\nu_e}}{dE_\nu} + (1 - P_m) \frac{dN_{\nu_x}}{dE_\nu}, \\ \frac{dN_{\nu_x}''}{dE_\nu} &\approx (1 - P_m) \frac{dN_{\nu_e}}{dE_\nu} + P_m \frac{dN_{\nu_x}}{dE_\nu} \end{aligned} \quad (9)$$

The parameter  $P_m$  depends not only on the mixing angles but also on the crossing probabilities PH and PL for the neutrino eigenstates at higher and lower resonances. It is also different for neutrinos and antineutrinos, but we will not elaborate further.

#### IV. THE TPC DETECTOR

It will be very interesting to see whether one can gain detailed information about the supernova neutrino spectrum(SN) and perhaps gain information about the neutrino hierarchy from a neutral current detector with high sensitivity.

To this end we are proposing to use a gaseous spherical TPC detector dedicated for SN neutrino detection through the neutrino-nucleus coherent process. More specifically to use a gaseous spherical TPC detector, dedicated to supernova neutrino detection, exploiting the neutrino-nucleus neutron coherent process. The first idea is to employ a a small size spherical TPC detector filled with a high pressure noble gas [8] [9]. Today the spherical detector is used for dark matter search at LSM (.6 m in diameter 10 bar pressure) underground laboratory and for NEWS experiment a future project at SNOLAB (1.5 m, 10 bar)[10]. Dark matter detector is focused in light-WIMP search using gas target of light elements as H, He and Ne are more sensitive in in the GeV and sub-GeV range, compared to current experiments using of Xe and Ge. During data taking the threshold was set at 30 eV, a second hint to reach low WIMP mass sensitivity.

For the SN project we could use a conceptual design of detector based on the existing technology and increase detector diameter and pressure to 50 bar taking into account recent developments. A key issue for such high-pressure operation is the use of a sensor ball smaller than the current 6.3 mm in diameter. In recent laboratory investigations we have successfully used 2 mm ball sensor. This is coming closer to our goal of 1 mm ball, which would be the ideal size for reaching stable operation at 50 bar. Using such small sensors will require lower operation voltage and therefore induce low electric field (E) at large distances:

$$E(r_1) = r_2 \frac{V_0}{r_1^2}$$

which shows that the electric field at the periphery is proportional to the radius of the small ball ( $r_2$ ) and inversely proportional to the radius square of the external sphere ( $r_1$ ). Such low field may become a concern for large detector. Clearly there is a contradiction between large detector and small sensor.

Recently we have successfully tested, however, a new idea with a multi-ball sensor which is supposed to solve this problem: The multi-ball system is employing many small conductive balls arranged around a larger spherical surface, that could also tune the electric field at large distance and at the same time could produce a segmentation of the detector. In the multi-ball arrangement the electric field at large distance is proportional to the distance of the balls from the center of the spherical detector and not to the radius of the balls as it is in the case of existing central single ball detector. Notice that such multi-ball system will optimize the electric field for any size of the external sphere and the detector segmentation will help to avoid pile-up events.

An enhancement of the neutral current component is achieved via the coherent effect of all neutrons in the target. Thus employing, e.g., Xe at 10 Atm, with a feasible threshold energy of about 100 eV in the recoiling nuclei, we show that one may expect, depending on the neutrino hierarchy, between 300 and 500 events for a sphere of radius 3m. This can go up to 1500 and 2500 events, if the pressure is raised at 50 Atm, something quite feasible to-day taking into account recent detector progress.

#### V. THE DIFFERENTIAL AND TOTAL CROSS SECTION

The differential cross section for a given neutrino energy  $E_\nu$  can be cast in the form[11]:

$$\left( \frac{d\sigma}{dT_A} \right)_w (T_A, E_\nu) = \frac{G_F^2 Am_N}{2\pi} (N^2/4) F_{coh}(T_A, E_\nu), \quad (10)$$

with

$$F_{coh}(T_A, E_\nu) = F^2(q^2) \left( 1 + \left( 1 - \frac{T_A}{E_\nu} \right)^2 - \frac{Am_N T_A}{E_\nu^2} \right) \quad (11)$$

where  $N$  is the neutron number and  $F(q^2) = F(T_A^2 + 2Am_N T_A)$  is the nuclear form factor. The effect of the nuclear form factor depends on the target (see Fig. 2).

Since the SN source is not "monochromatic" the above equation can be written as:

$$\frac{d\sigma}{dT_A} = \int_{E(T_A)}^{(E_\nu)_{\max}} \left( \frac{d\sigma}{dT_A} \right)_w (T_A, E_\nu) f_{sp}(E_\nu, T, a) dE_\nu \quad (12)$$

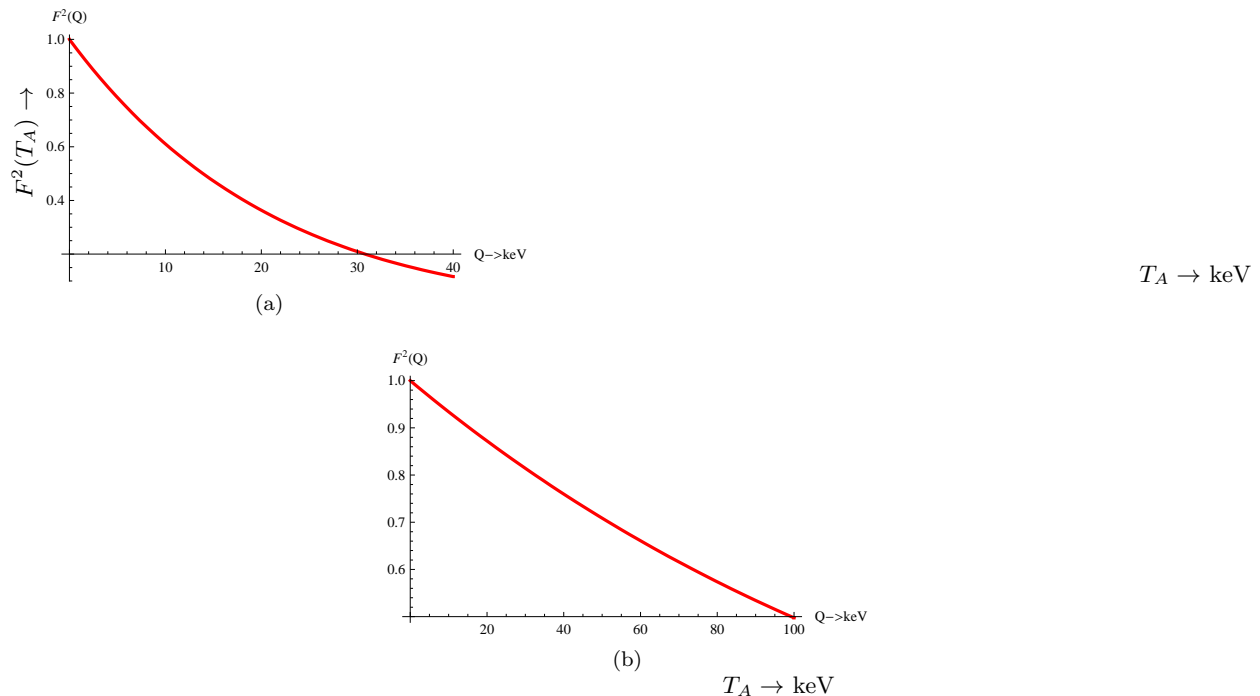


Figure 2: The square of the nuclear form factor,  $F^2(T_A)$ , as a function of the recoil energy for  $A=131$  (a) and  $A=40$  (b). Note that the maximum recoil energy is different for each target.

Where  $(E_\nu)_{\max}$  is the maximum neutrino energy and

$$E(T_A) = \frac{T_A}{2} + \sqrt{\frac{T_A}{2}(M_A + \frac{T_A}{2})}$$

Here  $(E_\nu)_{\max} = \infty$ .

Integrating the total cross section of Fig. 3 from  $T_A = E_{th}$  to infinity we obtain the total cross section. The threshold energy  $E_{th}$  depends on the detector.

The number of the observed events for each neutrino species is found to be:

$$N_{ev}(a, T) = \Phi_\nu(a, T) \sigma(a, T, E_{th}) N_N(P, T_0, R) \quad (13)$$

$$N_N(P, T_0, R) = \frac{P}{kT_0} \frac{4}{3} \pi R^3 \quad (14)$$

where  $N_N$  is the number of nuclei in the target, which depends on the pressure, ( $P$ ), the absolute temperature, ( $T_0$ ) and the radius  $R$  of the detector. We find:

$$N_N(P, T_0, R) = 1.04 \times 10^{30} \frac{P}{10 \text{ Atm}} \frac{300 \text{ K}}{T_0} \left( \frac{R}{10 \text{ m}} \right)^3 \quad (15)$$

### A. Results for the Xe target

The differential cross section for neutrino elastic scattering, obtained with the above neutrino spectrum, on the target  $^{131}_{54}\text{Xe}$  is shown in Fig. 3. Integrating the total cross section of Fig. 3 from  $T_A = 0$  to infinity we obtain the total cross section given in table IV. The above results refer to an ideal detector operating down to zero energy threshold. In the case of non zero threshold the event rate is suppressed as shown in Fig. 4.

Using Eq. 13 and the above total cross sections, after summing over all neutrino species (i.e. over all T), we obtain the number of events shown in Table V. It is a surprise for us that the total rate increases somewhat after the

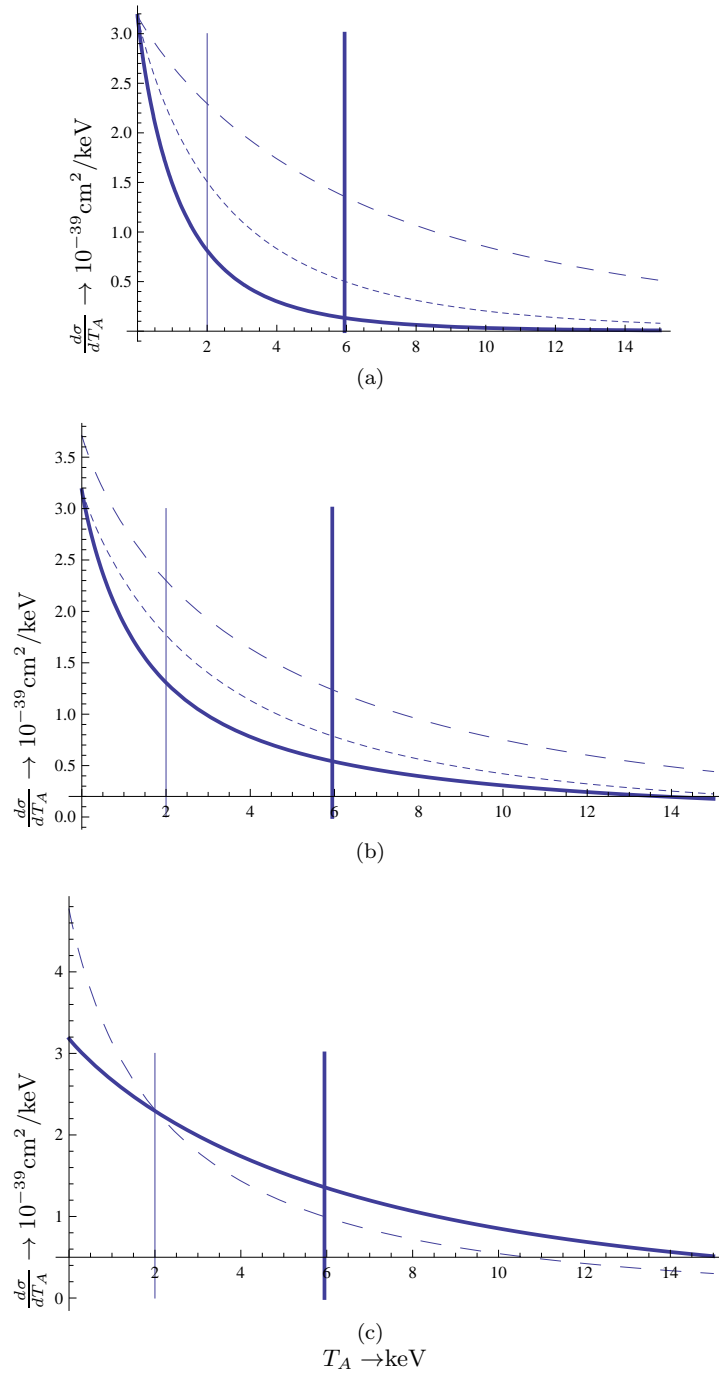


Figure 3: The differential cross section for elastic neutrino nucleus scattering in the case of the target  $^{131}_{54}\text{Xe}$  as a function of the recoil energy  $T_A$  in keV. In the case of a threshold energy of 2 keV, only the space on the right of the vertical bar is available. In the presence of quenching only the space on the right of the thick vertical bar is available. From top to bottom the primordial spectrum (a), the normal hierarchy (NH) (b) and inverted hierarchy (IH) (c) scenario. Otherwise the notation is the same as in Fig. 1

modification of the primary neutrino spectra. It is not shown here, but the  $e$  fraction of  $\nu_x$  is 77%, 65% and 46% for the S, NH and IH neutrino spectra respectively, i.e. it decreases as we go from the primary to the modified neutrino spectra. This is not relevant for a neutral current detector, but it may be an important element for detectors using the charged current process, so long as they are sensitive only to the  $\nu_e$  and  $\bar{\nu}_e$  components.

In the presence of a detector threshold of even 1 keV the above rates are reduced by about 20% (50%) in the absence

Table IV: The total neutrino nucleus cross section in the case of Xe target in units of  $10^{-39}\text{cm}^2$  assuming zero detector threshold.

$a$	$\sigma/10^{-39}\text{cm}^2$			
	$\nu_e$ T=3.5 MeV	$\tilde{\nu}_e$ T=5 MeV	$\sum_x \nu_x$ T=8 MeV	Total
0	4.117	8.312	19.764	32.194
0.75	4.361	8.815	20.921	34.097
1.50	4.749	9.608	22.727	37.083
2.00	5.104	10.330	24.346	39.780
3.00	6.074	12.288	28.621	46.083
4.00	7.408	14.966	34.147	56.521
5.00	9.118	18.364	40.546	68.028

Table V: The total event rate as a function of  $a$  in the case of a gaseous Xe target under a temperature 300  $^{\circ}\text{K}$  and various pressures with the indicated spherical detector radii. S, NH and IH stand for neutrino spectra in the standard (primary), modified in the NH and the IH neutrino respectively. These results were obtained by summing over all neutrino species assuming a zero detector energy threshold.

$a$	R=10m P=10Atm	R=10m P=10 Atm	R=10m P=10Atm	R=3m P=50Atm	R=3m P=50Atm	R=3m P=50Atm	R=4m P=10Atm	R=4m P=10Atm	R=4m P=10Atm
	S	NH	IH	S	NH	IH	S	NH	IH
0	10872	12275	15083	1467	1657	2036	695	785	965
0.75	11089	12520	15383	1497	1690	2076	709	801	984
1.5	11427	12901	15850	1542	1741	2139	731	825	1014
2.	11726	13238	16262	1583	1787	2195	750	847	1040
3.	12482	14089	17302	1685	1902	2335	798	901	1107
4.	13378	15093	18523	1806	2037	2500	856	965	1185
5.	14287	16108	19749	1928	2174	2666	914	1030	1263

(presence) of quenching.

### B. The Ar target

The differential cross for neutrino elastic scattering on the target  $^{40}_{18}\text{Ar}$  is shown in Fig. 5. For comparison we are currently calculating the differential cross sections to the excited states of  $^{40}\text{Ar}$  due to the neutral current. We also are going to calculate the charged current cross sections ( $\nu_e, e^-$ ) and ( $\tilde{\nu}_e, e^+$ ) on  $^{40}\text{Ar}$ , which are of interest in the proposal GLACIER, one of the large detectors<sup>1</sup>.

In the presence of a detector threshold of even 1 keV the above rates are reduced by about 10% (30%) in the absence (presence) of quenching.

### C. The Ne target

The differential cross for neutrino elastic scattering on the target  $^{20}_{10}\text{Ne}$  is shown in Fig. 7.

In the presence of a detector threshold of even 1 keV the above rates are reduced by about 5% (10%) in the absence (presence) of quenching.

<sup>1</sup> V. Tsakstara, private communication

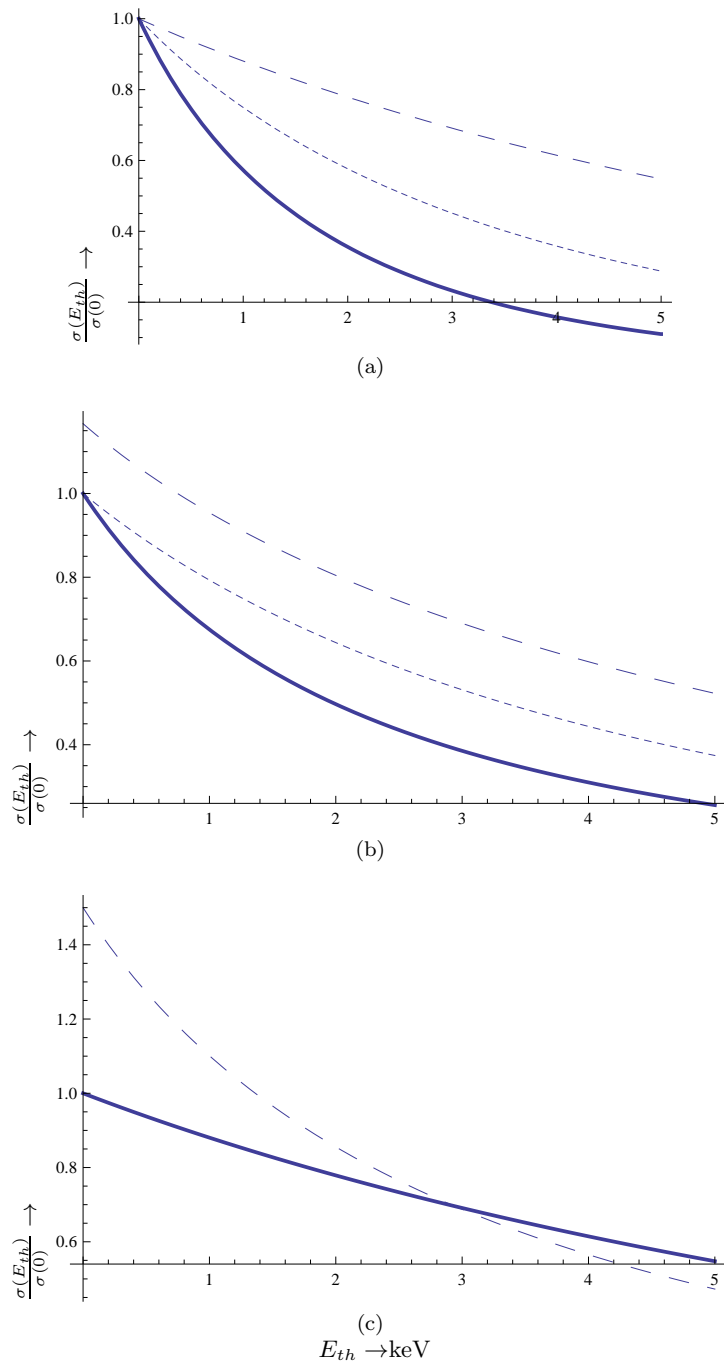


Figure 4: The ratio of the cross section at threshold  $E_{th}$  divided by that at zero threshold as a function of the threshold energy in keV in the case of a Xe target. From top to bottom the primordial spectrum (a), the normal hierarchy (NH) (b) and inverted hierarchy (IH) (c) scenario. Otherwise the notation is the same as in Fig. 1

## VI. CONCLUSIONS

From the above results one can clearly see the advantages of a gaseous spherical TPC detector dedicated for SN neutrino detection. The first idea is to employ a small size spherical TPC detector filled with a high pressure noble gas. An enhancement of the neutral current component is achieved via the coherent effect of all neutrons in the target. Thus employing, e.g., Xe at 10 Atm, with a feasible threshold energy of about 100 eV in the recoiling nuclei, one expects, depending on the neutrino hierarchy, between 300 and 500 events for a sphere of radius 3m. This can



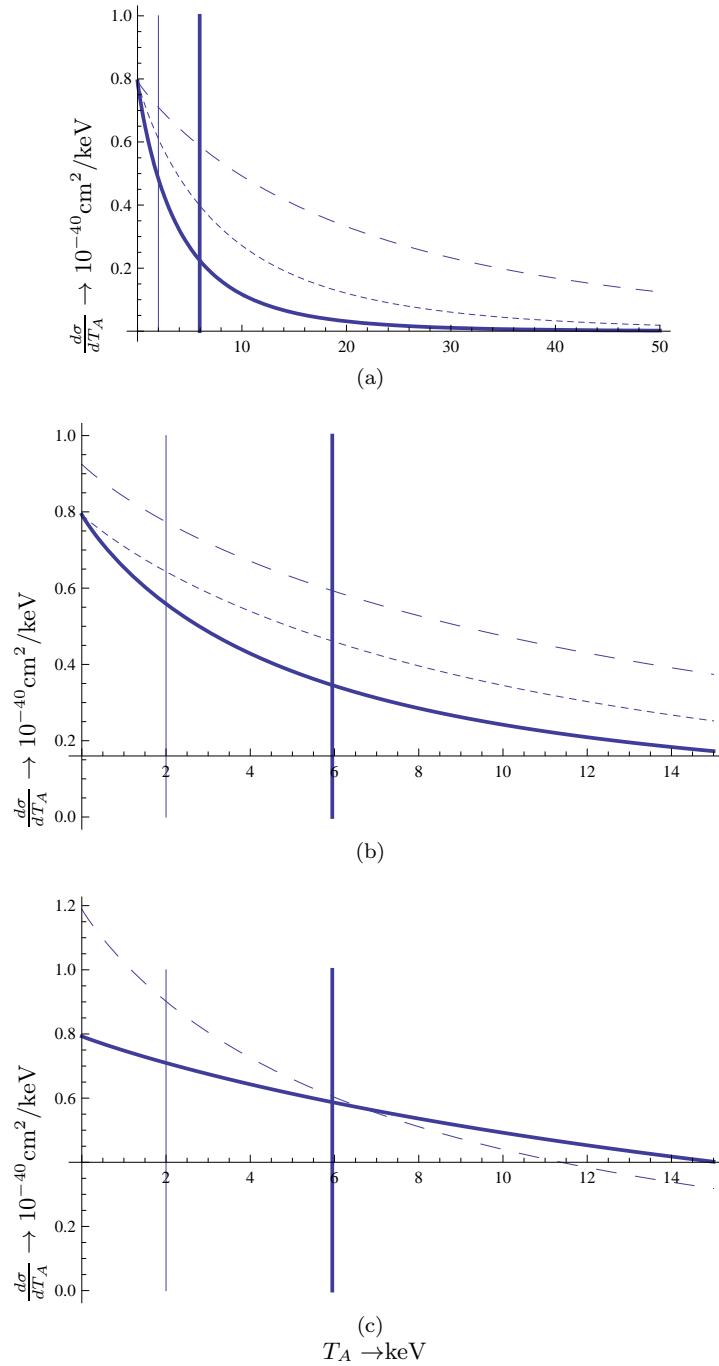


Figure 5: The same as in 3 in the case of the Ar target.

go up to 1500 and 2500 events if the pressure is raised at 50 Atm, something quite feasible even to-day. Employing  $^{40}\text{Ar}$  one expects between 150 and 200 events but it can become larger if the pressure can be increased above 50 Atm, something quite realistic.

The second idea is to build several such low cost and robust detectors and install them in several places over the world, utilizing the small radius spheres filled with Ar under relatively small pressure. The small low pressure spheres First estimates show that the required background level is modest and therefore there is no need for a deep underground laboratory. A mere 100 meter water equivalent coverage seems to be sufficient to reduce the cosmic muon flux at the required level (in the case of many such detectors in coincidence, a modest shield is sufficient). The maintenance of such systems, quite simple and needed only once every few years, could be easily assured by universities

Table VI: The total neutrino nucleus cross section in the case of Ar target in units of  $10^{-40}\text{cm}^2$  assuming zero detector threshold.

$a$	$\sigma/10^{-40}\text{cm}^2$			
	$\nu_e$ T=3.5 MeV	$\bar{\nu}_e$ T=5 MeV	$\sum_x \nu_x$ T=8 MeV	Total
0	3.324	6.520	13.678	23.521
0.75	3.525	6.908	14.412	24.845
1.50	3.843	7.518	15.528	26.888
2.00	4.133	8.067	16.497	28.693
3.00	4.917	9.537	18.905	33.359
4.00	5.990	11.488	21.690	39.168
5.00	7.353	13.843	24.480	45.676

Table VII: The same as in Table V in the case of the target  $^{40}\text{Ar}$ .

a	R=10m	R=10m	R=10m	R=3m	R=3m	R=3m	R=4m	R=4m	R=4m
	P=10Atm	P=10 Atm	P=10Atm	P=50Atm	P=50Atm	P=50Atm	P=10Atm	P=10Atm	P=10Atm
	S	NH	IH	S	NH	IH	S	NH	IH
0	777	874	1070	104	118	144	49	55	68
0.75	789	889	1087	106	120	146	50	56	69
1.5	808	910	1113	109	122	150	51	58	71
2.	824	928	1134	111	125	153	52	59	72
3.	861	968	1182	116	130	159	55	61	75
4.	895	1005	1225	120	135	165	57	64	78
5.	920	1031	1254	124	139	169	58	66	80

or even by secondary schools, with only specific running programs. Admittedly such a detector scheme, measuring low energy nuclear recoils from neutrino nucleus elastic scattering, will not be able to determine the incident neutrino vector and, therefore, it is not possible to localize the supernova this way. This can be achieved by a cluster of such detectors in coincidence by a triangulation technique.

A network of such detectors in coincidence with a sub-keV threshold could also be used to observe unexpected low energy events. This low energy range has never been explored using massive detectors. A challenge of great importance will be the synchronization of such a detector cluster with the astronomical  $\gamma$ -ray burst telescopes to establish whether low energy recoils are emitted in coincidence with the mysterious  $\gamma$  bursts.

In summary: networks of such dedicated gaseous TPC detectors, made out of simple, robust and cheap technology, can be simply managed by an international scientific consortium and operated by students. This network comprises a system, which can be cheaply maintained for several decades (or even centuries). Obviously this is a key point towards preparing to observe few galactic supernova explosions.

Thus with adequate funding and if we are lucky to soon have a supernova not much further than 10 kps, we might be able to observe supernova neutrinos. This event, in conjunction with organizing an activity to honor Gerry, will be a tribute to to G. E. Brown for the memorable work he did on the equation of state of collapsing stars, in collaboration with another giant of physics, H. Bethe. Among other things they contributed to the understanding of the birth of our supernova neutrinos.

### Acknowledgement

JDV would like to acknowledge support by ARC Centre of Excellence in Particle Physics at the Terascale, University of Adelaide, and thank Professor A. W. Thomas for his hospitality. He would also like to express his appreciation to Tom Kuo for providing the opportunity to dedicate this work to the unforgettable Gerry.

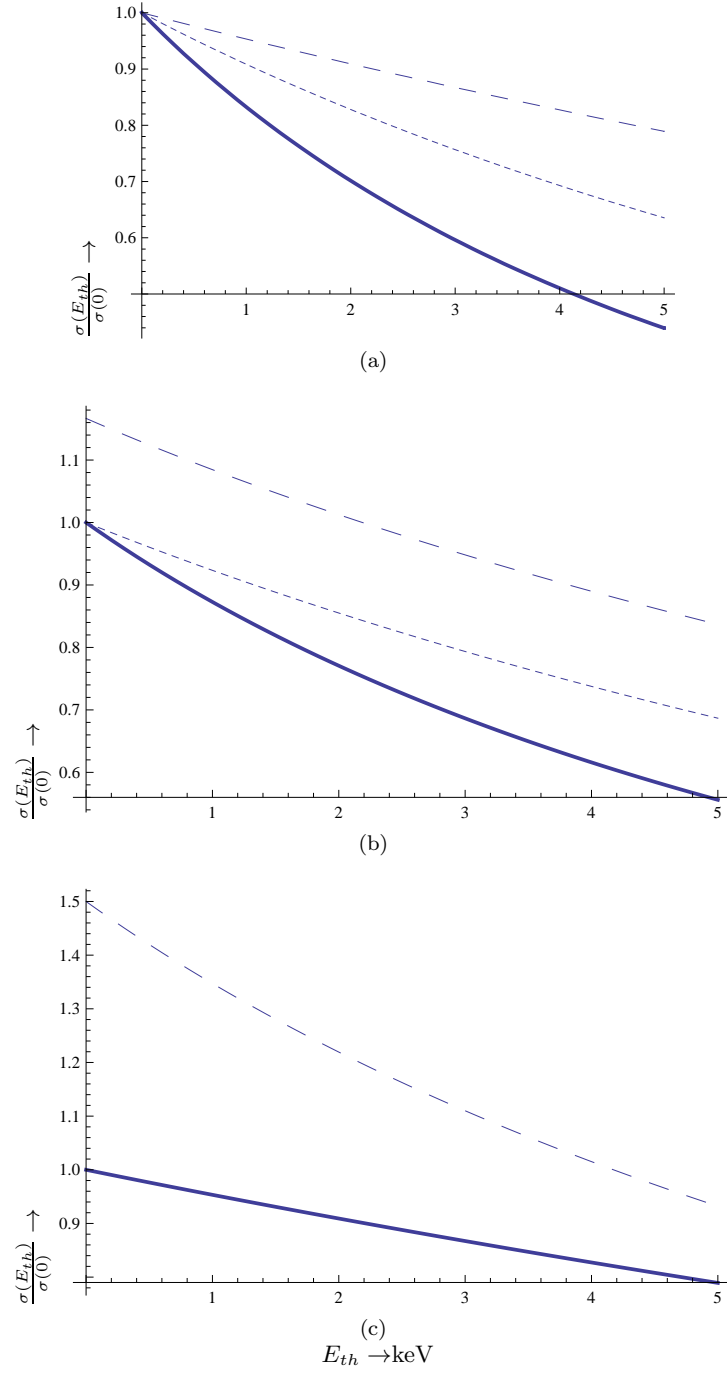


Figure 6: The same as in Fig. 4 in the case of the Ar target

### References

- 
- [1] R. Tomas, M. Kachelriess, A. G.G. Raffelt, A. Janka, and L. Schreck, JCAP **0409**, 015 (2004).  
 [2] H. T. Janka, K. Langanke, A. Marek, G. Martinez-Pinedo, and B. Mueller, Phys. Rep. **442**, 38 (2007), arXiv:astro-ph/0612072 [pdf, ps, other].

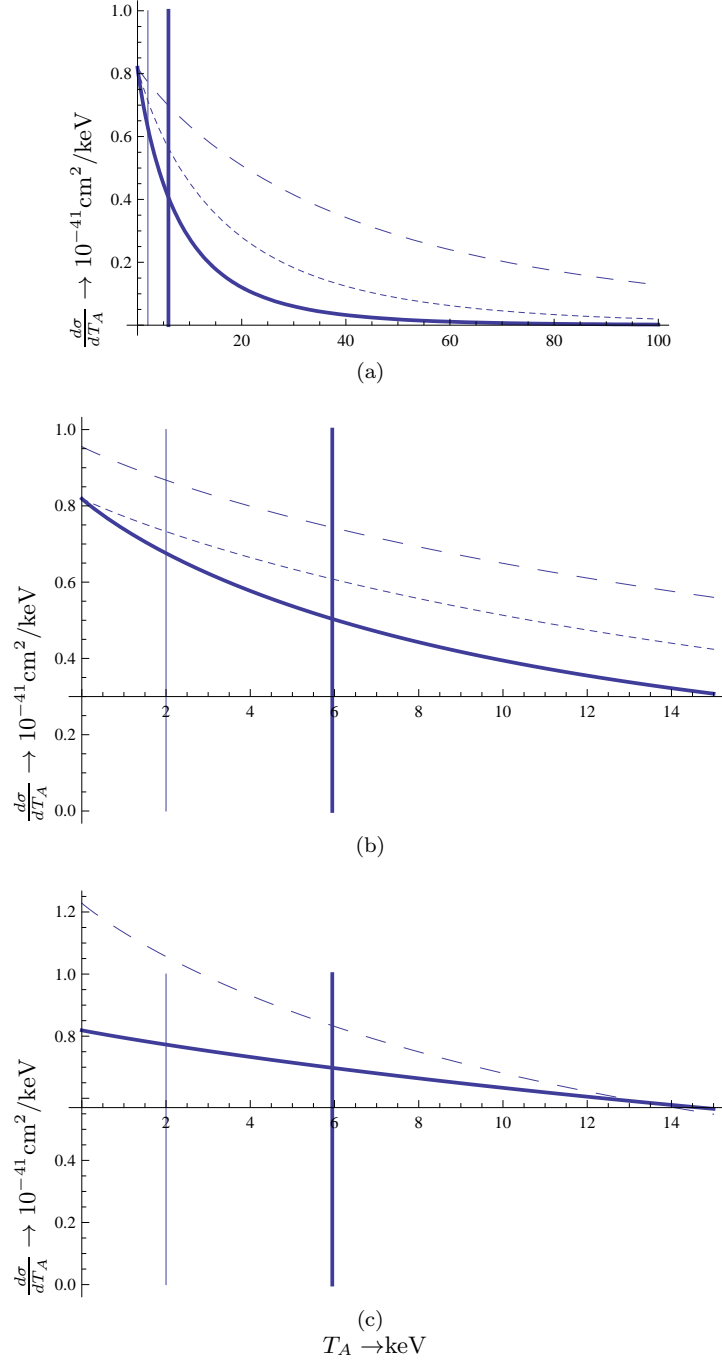


Figure 7: The same as in 3 in the case of the Ne target.

- [3] A. S. Dighe and A. Y. Smirnov, Phys. Rev. D **62**, 033007 (2000).
- [4] K. Nakazato, E. Moshida, Y. Nino, and H. Suzuki, Astrophys. J. **804**, 75 (2015), arXiv:1503.01236 (astro-ph.HE).
- [5] L. Wolfenstein, Phys. Rev. D **17**, 2369 (1978).
- [6] S. P. Mikheev and A. Y. Smirnov, Sov. J. Nucl. Phys. **42**, 913 (1985), yad. Fiz. 42, 1441 (1985).
- [7] S. H. Chiu, C.-C. Huang, and K.-C. Lai, Prog. Theor. Exp. Phys. p. 063V01 (2015), arXiv:1312.4262 (hep-ph).
- [8] I. Giomataris et al., JINST **3**, P09007 (2008).
- [9] E. Bougamont et al., J. Mod. Phys. **3**, 57 (2012).
- [10] G. Gerbier, I. Giomataris, P. Magnier, A. Dastgheibi, M. Gros, D. Jourde, E. Bougamont and X. F. Navick et al., arXiv:1401.7902 [astro-ph.IM].
- [11] Y. Giomataris and J. Vergados, Phys. Lett. **B 634**, 23 (2006).

Table VIII: The total neutrino nucleus cross section in the case of Ne target in units of  $10^{-41}\text{cm}^2$  assuming zero detector threshold.

$a$	$\sigma/10^{-41}\text{cm}^2$			
	$\nu_e$ T=3.5 MeV	$\bar{\nu}_e$ T=5 MeV	$\sum_x \nu_x$ T=8 MeV	Total
0	6.861	13.456	28.232	48.548
0.75	7.277	14.258	29.747	51.281
1.50	7.934	15.515	32.049	55.497
2.00	8.531	16.649	34.049	59.229
3.00	10.150	19.683	39.021	68.854
4.00	12.364	23.708	44.772	80.844
5.00	15.176	28.568	50.537	94.281

Table IX: The same as in Table V in the case of the target  $^{20}\text{Ne}$ .

a	R=10m	R=10m	R=10m	R=3m	R=3m	R=3m	R=4m	R=4m	R=4m
	P=10Atm S	P=10 Atm NH	P=10Atm IH	P=50Atm S	P=50Atm NH	P=50Atm IH	P=10Atm S	P=10Atm NH	P=10Atm IH
0	160	180	220	21	24	29	10	11	14
0.75	163	183	224	22	24	30	10	11	14
1.5	166	187	229	22	25	31	10	12	14
2.	170	191	234	22	25	31	10	12	14
3.	177	199	243	23	26	32	11	12	15
4.	184	207	253	24	28	34	11	13	16
5.	190	213	258	25	28	34	12	13	16

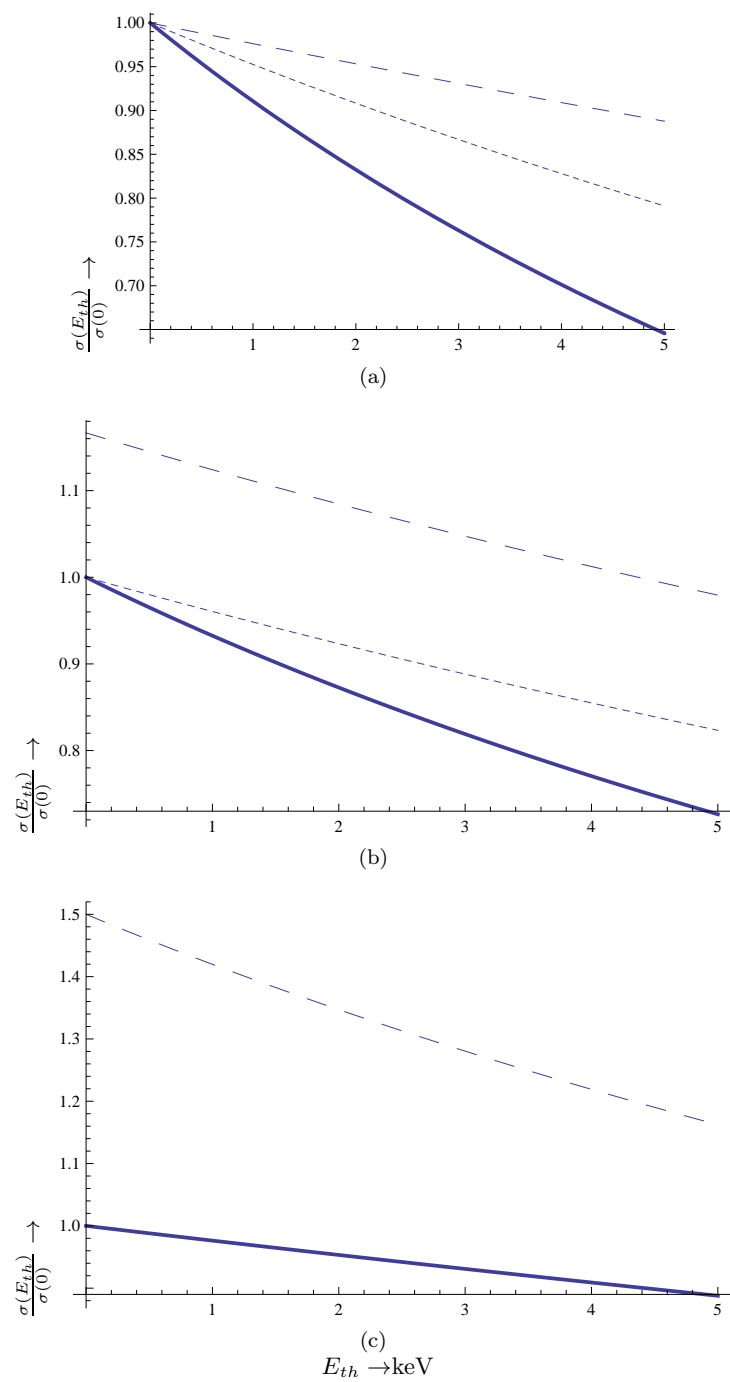


Figure 8: The same as in Fig. 4 in the case of the Ne target.